Mechanistic dissection of premature translation termination induced by acidic residues-enriched nascent peptide
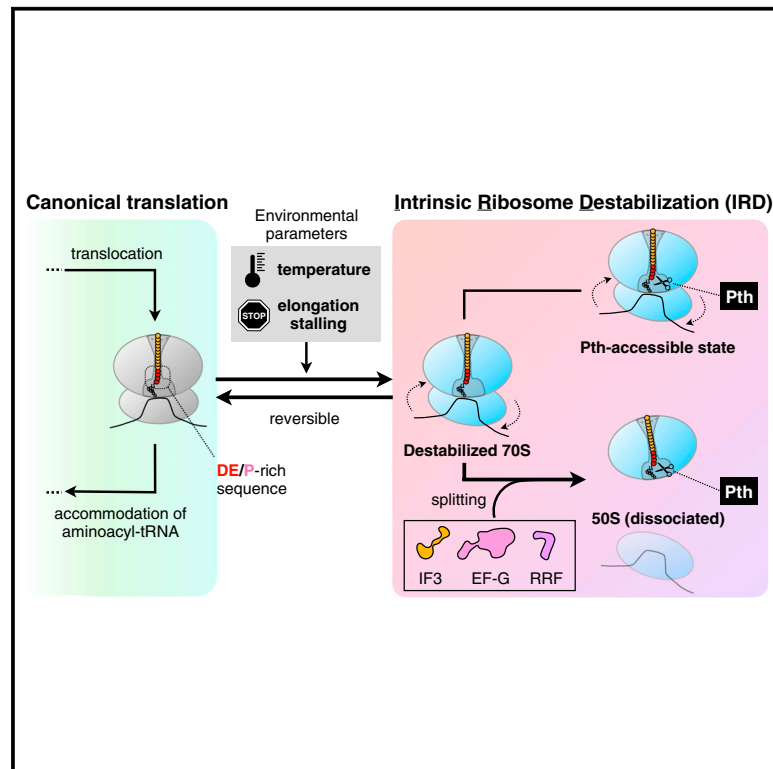
Graphical abstract

Highlights

- Temperature and elongation stalling affect the intrinsic destabilization of the ribosome

- Intrinsically destabilized ribosomes are not necessarily split into subunits

- Pth hydrolyzes the peptidyl-tRNA within the destabilized 70S without ribosome splitting

- Ribosome recycling factors can split the destabilized 70S ribosome with peptidyl-tRNA

Authors

Yuhei Chadani, Takashi Kanamori, Tatsuya Niwa, Kazuya Ichihara, Keiichi I. Nakayama, Akinobu Matsumoto, Hideki Taguchi

Correspondence

ychadani@okayama-u.ac.jp (Y.C.), taguchi@bio.titech.ac.jp (H.T.)

In brief

Chadani et al. characterize the molecular determinants of acidic-rich nascent chain-induced intrinsic ribosome destabilization (IRD) in *Escherichia coli*. IRD is affected by temperature, elongation stalling, and translation factors. IRD prematurely terminates translation through two distinct mechanisms: either Pth-mediated hydrolysis of peptidyl-tRNA within 70S complex or splitting facilitated by recycling factors.

Cell Reports

Article

Mechanistic dissection of premature translation termination induced by acidic residues-enriched nascent peptide

Yuhei Chadani,[1,8,*] Takashi Kanamori,[2] Tatsuya Niwa,[3,4] Kazuya Ichihara,[5] Keiichi I. Nakayama,[6,7] Akinobu Matsumoto,[5] and Hideki Taguchi[3,4,*]

[1]Faculty of Environmental, Life, Natural Science and Technology, Okayama University, Okayama 700-8530, Japan
[2]GeneFrontier Corporation, Kashiwa-shi, Chiba 277-0005, Japan
[3]Cell Biology Center, Institute of Innovative Research, Tokyo Institute of Technology, Yokohama 226-8503, Japan
[4]School of Life Science and Technology, Tokyo Institute of Technology, Yokohama 226-8503, Japan
[5]Division of Biological Science, Graduate School of Science, Nagoya University, Nagoya 464-8602, Japan
[6]Anticancer Strategies Laboratory, TMDU Advanced Research Institute, Tokyo Medical and Dental University, Bunkyo-ku, Tokyo 113-8510, Japan
[7]Division of Cell Biology, Medical Institute of Bioregulation, Kyushu University, Fukuoka 812-8582, Japan
[8]Lead contact
*Correspondence: ychadani@okayama-u.ac.jp (Y.C.), taguchi@bio.titech.ac.jp (H.T.)
https://doi.org/10.1016/j.celrep.2023.113569

SUMMARY

Ribosomes polymerize nascent peptides through repeated inter-subunit rearrangements between the classic and hybrid states. The peptidyl-tRNA, the intermediate species during translation elongation, stabilizes the translating ribosome to ensure robust continuity of elongation. However, the translation of acidic residue-rich sequences destabilizes the ribosome, leading to a stochastic premature translation cessation termed intrinsic ribosome destabilization (IRD), which is still ill-defined. Here, we dissect the molecular mechanisms underlying IRD in *Escherichia coli*. Reconstitution of the IRD event reveals that (1) the prolonged ribosome stalling enhances IRD-mediated translation discontinuation, (2) IRD depends on temperature, (3) the destabilized 70S ribosome complex is not necessarily split, and (4) the destabilized ribosome is subjected to peptidyl-tRNA hydrolase-mediated hydrolysis of the peptidyl-tRNA without subunit splitting or recycling factors-mediated subunit splitting. Collectively, our data indicate that the translation of acidic-rich sequences alters the conformation of the 70S ribosome to an aberrant state that allows the noncanonical premature termination.

INTRODUCTION

The ribosome, the central factory of the cellular proteome, is composed of the large and small subunits. In bacteria such as *Escherichia coli*, more than 50 ribosomal proteins and three ribosomal RNAs (rRNAs) are assembled into the large and small subunits. These subunits associate to form the 70S complex (80S in eukaryotes) at the initiation codon of the mRNA and start the polymerization of amino acids. The stable association between the large and small subunits throughout translation elongation is a prerequisite for the synthesis of the intact, complete proteins specified by the open reading frames (ORFs).

The ribosome undergoes dynamic structural rearrangements during mRNA translation. EF-Tu (eEF1 in eukaryotes) delivers the aminoacyl-tRNA (aa-tRNA) that is cognate with the mRNA codon within the ribosomal A-site. After verification of the correct codon-anticodon interaction in the decoding center of the small subunit, EF-Tu dissociates from the ribosome, and the aa-tRNA is accommodated in the ribosome with the acceptor amino acid residue placed in the peptidyl transfer center (PTC). The PTC of

the ribosome then catalyzes the transpeptidation reaction between the aminoacyl-tRNA within the A-site and the peptidyl-tRNA within the P-site. After transpeptidation, a ratchet-like relative rotation of the small and large subunits occurs, forming the so-called "hybrid" state conformation of the ribosome and translocating the one residue-extended peptidyl-tRNA from the A-site to the P-site, and the ribosome moves one codon ahead. The action of EF-G (eEF2) increases the fidelity and efficiency of the translocation process; however, biochemical and structural analyses have shown that the ratchet-like rotation spontaneously occurs even in the absence of EF-G.[1,2] In contrast, this spontaneous ratcheting is suppressed when the peptidyl-tRNA is located within the P-site of the ribosome in the "classic" conformational state.[3] This "locking" would prevent futile conformational rearrangements that could trigger translational errors.[4]

The nascent peptide continuously moves into and through the ribosomal exit tunnel as it gains amino acid residues, one by one, at the PTC. The exit tunnel accommodates and interacts with 30~40 amino acids of the extended nascent peptide chain and regulates the various functions of the ribosome.[5] Several studies

have pointed out that the 70S ribosome bearing a peptidyl-tRNA is more stable than the vacant one.[6–12] Furthermore, the peptidyl-tRNA also prevents the premature abortion of translation by the recycling factors-mediated splitting of the translating ribosome complex.[13–15] Taken together with the "locking" model mentioned above, these lines of evidence indicate that the peptidyl-tRNA is not simply a translation intermediate, but it functions to ensure the continuity of translation elongation. This feature of the peptidyl-tRNA would ensure robust protein synthesis under the stressful conditions that impact ribosome stability, such as a low Mg^{2+} ion concentration[16] and high temperature.[17–20]

However, certain kinds of nascent peptides threaten the continuity of translation elongation. The translation of sequences enriched in negatively charged residues destabilizes the ribosome, stochastically aborting the translation in a stop codon-independent manner, in a phenomenon termed intrinsic ribosome destabilization (IRD).[21] Such IRD-inducing sequences are widespread among about half of the annotated ORFs in various bacterial species.[22]

We have also shown that IRD can be harnessed for environmental sensing.[21] For instance, *E. coli mgtL*, a regulatory upstream ORF of *mgtA* (encoding a Mg^{2+} transporter), harbors the "EPDP" IRD sequence adjacent to the initiation codon. The intracellular Mg^{2+} concentrations affect the stability of the ribosome translating the EPDP sequence. As a result, the expression of MgtA becomes Mg^{2+} dependent,[21] meaning that IRD has a potential to be integrated into a survival strategy of bacteria.

As shown in the *mgtL* case, IRD sequences encoded within the first 30–40 codons of ORFs frequently abort translation, whereas those more distant from the start codons do so only poorly. This difference depends on the presence or absence of the tunnel-traversing nascent chain, which tethers the subunits. IRD counteraction by nascent chains depends on their ''length'' within the tunnel and ''bulkiness'' near the entrance of the tunnel, suggesting that nonspecific, but more frequent interactions stabilize the ribosome complex.[22] These findings imply that the sophisticated design of the ribosomal exit tunnel minimizes the risk of acidic residue-rich sequences to expand the repertoire of synthesizable polypeptides.

Recently, we found that eukaryotic ribosomes are also destabilized by the translation of an acidic residue-rich sequence.[23] IRD in eukaryotes shares some similarities with that in prokaryotes; e.g., the tunnel-accommodated nascent chain counteracts IRD in a length-dependent manner. However, we also detected a difference in IRD between eukaryotes and prokaryotes. In a reconstituted eukaryotic translation system, the IRD irreversibly inactivates the translation elongation but does not necessarily split the 80S complex into the subunits. In contrast, our previous study using a reconstituted *E. coli* translation system (PURE system) showed that the 70S ribosome dissociates into the subunits during the translation of a polyacidic sequence.[21] This difference motivated us to determine how IRD prematurely terminates translation in *E. coli*.

In this study, we evaluated the influences of translation factors, ribosome components, and environmental parameters on IRD to dissect the elementary processes of the nascent chain-dependent destabilization of the *E. coli* ribosome complex. We found that IRD depends heavily on temperature and elongation stalling.

These features allowed us to reconstitute the IRD phenomenon using the 70S ribosome, free from other translation factors. Further analyses revealed that intrinsically destabilized ribosomes are not necessarily split as well as in eukaryotes and could prematurely terminate elongation by two independent mechanisms: (1) peptidyl-tRNA hydrolase (Pth)-mediated hydrolysis of peptidyl-tRNAs within the 70S complex or (2) subunit splitting by IF3, EF-G, and ribosome recycling factor (RRF) without translation termination. These suggest that acidic nascent peptide alters the conformation of the 70S complex to an aberrant state that allows the normally improbable reactions on the translating ribosome.

RESULTS

EF-G action is involved in IRD

Since IRD occurs during translation elongation, we focused on the EF-G-catalyzed translocation of peptidyl-tRNA, which involves the most dynamic structural rearrangements in the ribosome complex.[24] A model mRNA encoding 10 consecutive glutamates (10E) in the middle of an ORF (*E. coli* Maa −10E)[21] was translated by the S30 lysate in the presence of excess EF-G (10 μM, Figure 1A). The addition of wild-type EF-G increased the amount of premature product in a 10E motif-dependent manner (Figures 1A and 1B). On the contrary, EF-G lacking domain IV, which is critical for the effective translocation of peptidyl-tRNA,[25,26] did not appreciably affect IRD (Figures 1A and 1B). These results indicate that EF-G participates in the IRD phenomenon.

We also tested the influence of EF-G on IRD in living *E. coli* cells. To conditionally deplete the functional EF-G, which is essential for *E. coli*, we used EF-G G502D mutant (*fusA*[ts]).[27] Subsequently, the *mgtL-lacZ* translational fusion reporter was expressed, and IRD frequency was evaluated as the translation continuation (TC) frequency of *mgtL* (TC index, calculated as LacZ activity ratios [(DEP+)/(no DEP)]).[22] Notably, the frequency of IRD decreased at the non-permissive temperature (42°C, Figure 1C, panel 1). Conversely, increased EF-G promoted IRD (Figure 1C, panel 2). EF-G also affected the expression of MgtA, which is strongly dependent on the translation of *mgtL* (Figures S1A and S1B). These results again show that EF-G is involved in the occurrence of IRD.

Ribosome stalling (pausing) enhances IRD

Involvement of EF-G motivated us to examine whether ET-Tu, another elongation factor, also has an influence on IRD. The 3D-*lacZ* or 3E-*lacZ* mRNA was translated by a reconstituted *in vitro* translation system, the PURE system (PURE*frex* v1.0), in the presence of various concentrations of EF-Tu. A decline of EF-Tu significantly increased the frequency of IRD (Figures 2A and S2A).

Scarcity of EF-Tu causes the decline of the delivery of aminoacyl-tRNAs, resulting in the ribosome stalling. This raises an interesting possibility that IRD could be enhanced by ribosome stalling (Figure 2B). To examine this hypothesis, we induced ribosome stalling by several approaches. We used truncated mRNAs (nonstop mRNAs), which cause ribosome stalling at the 3′ end in the absence of ribosome rescue factors such as
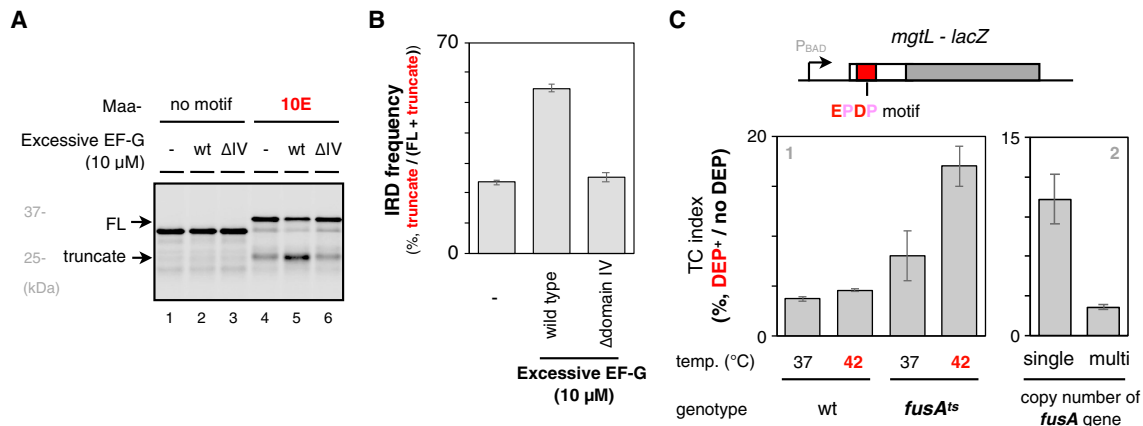
Figure 1. EF-G is involved in IRD in a translocation-independent manner

(A and B) Excessive amounts of EF-G enhance IRD. The Maa-LacZα (no motif) and Maa-10E sequence[21] was translated by the S30 lysate *in vitro* translation system in the presence of ^{35}S-methionine (A). Final 10 μM of purified EF-G and EF-G Δdomain IV mutant were added where indicated. The frequency of IRD-dependent premature termination was calculated as the ratio of the full-length product and the truncated product prematurely terminated in the 10E sequence (B) (#).

(C) Upper: the *mgtL-lacZ* reporter, which enables the evaluation of the IRD frequency at an N-terminal IRD-prone motif (EPDP) by comparison with its derivatives harboring the DE/P-substitution in *mgtL* (no DEP).[21,22] Panel 1: these reporter genes were individually expressed in *E. coli* ECY725 (WT) and its *fusA*[ts] (G502D)[27] derivative strains at the permissive (37°C) or non-permissive temperature (42°C) for measurements of β-galactosidase activities (m.u.), respectively. The downstream translation efficiency, subjected to the IRD downregulation, was then calculated as the LacZ activity ratio (DEP[+]/no DEP), termed the translation continuation (TC) index. Panel 2: the TC indices of the *mgtL-lacZ* within *E. coli* harboring the plasmid without (single) or with the *rpsL-rpsG-fusA-tufA* operon (multi) (#). Note that extra expression of EF-G from plasmids showed no distinguishable difference in the growth of *E. coli*. (#): the mean values ± SE estimated from three biological replicates (n = 3) are shown.

tmRNA-SmpB and ArfA.[28] The GFP-10X nonstop (ns) mRNAs (GFP-10X-ns: X stands for Asp: D, Glu: E, Lys: K, or Arg: R, as summarized in Figure 2C) were translated by the PURE system without any rescue factors. The translation products of nonstop mRNA accumulated exclusively as peptidyl-tRNAs for all the constructs examined (Figure 2D, lanes 1, 4, 7, and 10, "full-length" control experiments without mRNA truncation are shown in Figure S2B). The peptidyl-tRNAs produced from GFP-10K and GFP-10R mostly resisted Pth, indicating that the stalled ribosome accommodating the 10K or the 10R peptidyl-tRNA is structurally stable, and Pth cannot access the ester linkage of peptidyl-tRNA (Figure 2D, lanes 7–12; Figure 2E). In contrast, the GFP-10D and GFP-10E peptidyl-tRNAs were completely cleaved by Pth, indicating that the ribosome structure was somehow altered when the stalled complex contained IRD-inducing sequences (Figure 2D, lanes 1–6; Figure 2E). It is noteworthy that the sensitivity to Pth was correlated with the number of the acidic residues (Figure S2C). In addition, IRD was enhanced even when the ribosome stalled in the middle of the mRNA, excluding the possibility that the promotion of IRD is specific to the 3' end of nonstop mRNAs (Figures S2D–S2F). These findings suggest that the stalled ribosomes with the vacant A-site (classic state) are susceptible to intrinsic destabilization. Moreover, the prominent occurrence of IRD with the stalled ribosome, in which the translocation of peptidyl-tRNA does not occur, argues against the dependence of IRD on the EF-G-catalyzed canonical "translocation."

The ribosome resists IRD at low temperatures

Previous studies showed that not only the Mg^{2+} concentration but also the temperature influence the stability of the ribosome complex.[17–20] Accordingly, we next examined whether IRD depends on temperature. We translated the GFP-10E mRNA using the PURE system at either 37°C or 20°C and observed little accumulation of abortive peptidyl-tRNA at 20°C (Figure 3A). Furthermore, translation of GFP-10E-nonstop (ns) mRNA at 20°C altered the properties of the accumulated peptidyl-tRNA compared to that at 37°C because it was partially resistant to Pth and partially sensitive to puromycin. (Figure 3B). Of note, Pth and puromycin had sufficient activities at 20°C and even at 4°C (Figures S3A–S3C). Thus, the properties of the ribosomes stalled at the IRD sequence at 20°C would be different from those of the ribosomes stalled at 37°C, at which they are significantly destabilized (Figure 3B, lanes 1–4). In contrast, minimal catalytic alternation of the ribosome was observed when they stalled on the polybasic (10R) nonstop mRNA (Figure 3C). Considering the acidic residues-specific inverse temperature profiles of the Pth and puromycin sensitivities (Figures S3D and S3E), it is likely that the ribosomes translating an IRD sequence maintain the intact 70S structure at low temperatures.

We next examined whether the stabilization of the 70S complex at the low temperature is reversible. To assess the reversibility, the GFP-10E-ns mRNA was translated by the PURE system at 20°C, and further translation was stopped by the addition of spectinomycin, which does not alter the occurrence of IRD (Figures S3F and S3G). The reaction mixture was then incubated at 37°C in the presence of Pth or puromycin (Figure 3D). As expected, the shift from low (20°C) to high (37°C) temperature destabilized the ribosome that had translated the GFP-10E-ns mRNA (Figure 3D, panels 1 and 2). In contrast, the shift from 37°C to 20°C did not alter the proportions of Pth- or puromycin-reactive peptidyl-tRNAs (Figure 3D, panels 3
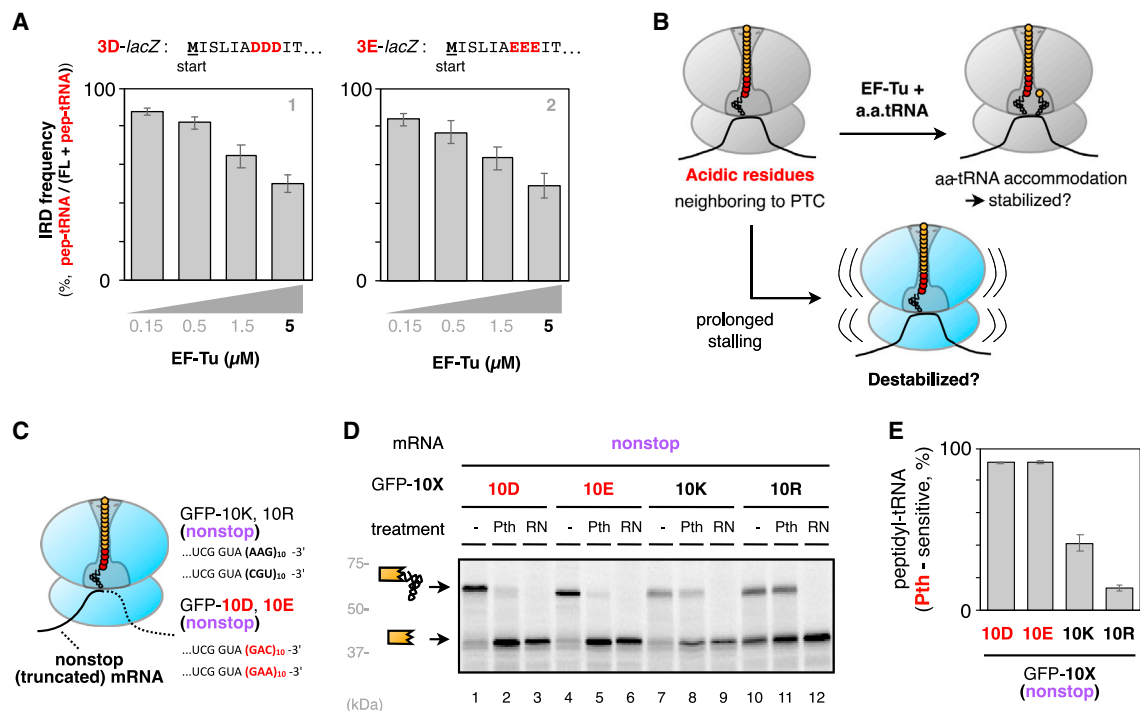
Figure 2. Translational stalling/pausing enhances IRD

(A) The amount of EF-Tu is inversely correlated with the IRD efficiency. The 3D- and 3E-*lacZ* mRNAs, encoding the acidic tripeptide motif near the N terminus, were translated by the PURE system (PURE*frex* v1.0) containing 5, 1.5, 0.5, and 0.15 μM of EF-Tu. The IRD efficiency was calculated from the proportion of the peptidyl-tRNA (pep-tRNA) and the full-length polypeptide chain, as shown in Figure S2A (#).

(B) A plausible model based on the EF-Tu experiment. The ribosome that stalled due to the shortage of EF-Tu should accommodate the peptidyl-tRNA within the P-site, while the A-site is vacant.

(C) Schematic of the ribosome stalled at the 3′ end of GFP-10X nonstop mRNA. Nucleotide sequences of 10K, 10R, 10D, and 10E nonstop mRNAs are shown.

(D) The GFP-10D (lanes 1–3), -10E (lanes 4–6), -10K (lanes 7–9), and -10R (lanes 10–12) nonstop mRNAs were translated by PURE*frex*. Translation products were labeled with Cy5-Met-tRNA, as described previously.[21] Samples were treated with peptidyl-tRNA hydrolase (Pth) as indicated and separated by neutral pH SDS-PAGE with optional RNase A (RN) pretreatment. The peptidyl-tRNA and tRNA-released truncated peptide are schematically indicated.

(E) The ratio of the GFP-10X peptidyl-tRNA that was sensitive to Pth, calculated as described in the STAR Methods (#). (#): the mean values ± SE estimated from three independent technical replicates (n = 3) are shown.

and 4). This indicates that IRD occurring at 37°C under the PURE system translation is an irreversible phenomenon.

IRD allows Pth to hydrolyze the peptidyl-tRNA associated with the 70S ribosome complex.

To directly assess the influence of temperature on IRD, the ribosomes translating GFP-10E-ns mRNA were fractionated by sucrose density gradient (SDG) ultracentrifugation (preliminary experiments in Figures S4A–S4C). At 37°C, most GFP-10E-ns peptidyl-tRNA was associated with the 70S complex, while 24% was associated with the 50S subunit (Figure 4A, panel 2, red line). Strikingly, the peptidyl-tRNA associated with the 50S subunit was decreased to 11% at low temperatures (20°C, Figure 4A, panel 2, blue line) or to 8% when the 10E motif was replaced with the 10R polybasic motif (Figure 4A, panel 3, red line). This tendency was reproduced even when conducting the assay using the bL31-truncated ribosome (Figure S4D), which is more prone to induce IRD.[21] These results support our hypothesis that the 70S integrity is better preserved at 20°C, even when it contains an IRD-evoking peptidyl-tRNA.

While observing a low-temperature-dependent stabilization of the 70S complex, unlike our previous results using the bL31-

truncated ribosome,[21] the majority of GFP-10E-ns peptidyl-tRNAs remained associated with the 70S complex at 37°C. This raises the question of whether these 70S complexes are intrinsically destabilized. Noteworthy, the GFP-10E peptidyl-tRNAs associated with the 70S complex at 37°C were completely cleaved upon Pth treatment (Figure 4B). This result indicates that, similar to what has been observed in eukaryotes,[23] the destabilized prokaryotic ribosomes may undergo Pth-induced hydrolysis of peptidyl-tRNA without subunit splitting.

Acidic nascent peptide induces reversible and spontaneous destabilization of the 70S ribosome complex

To investigate the destabilization of the 70S ribosome complex further, the 70S complexes accommodating the GFP-10E-ns peptidyl-tRNA within, prepared at 20°C, were isolated by SDG fractionation. The isolated 70S complexes (Figure 5A, the "isolated 70S" hereafter) can catalyze transpeptidation to puromycin as well as stop codon-independent translation termination in conjunction with the alternative ribosome rescue factors,[29–33]
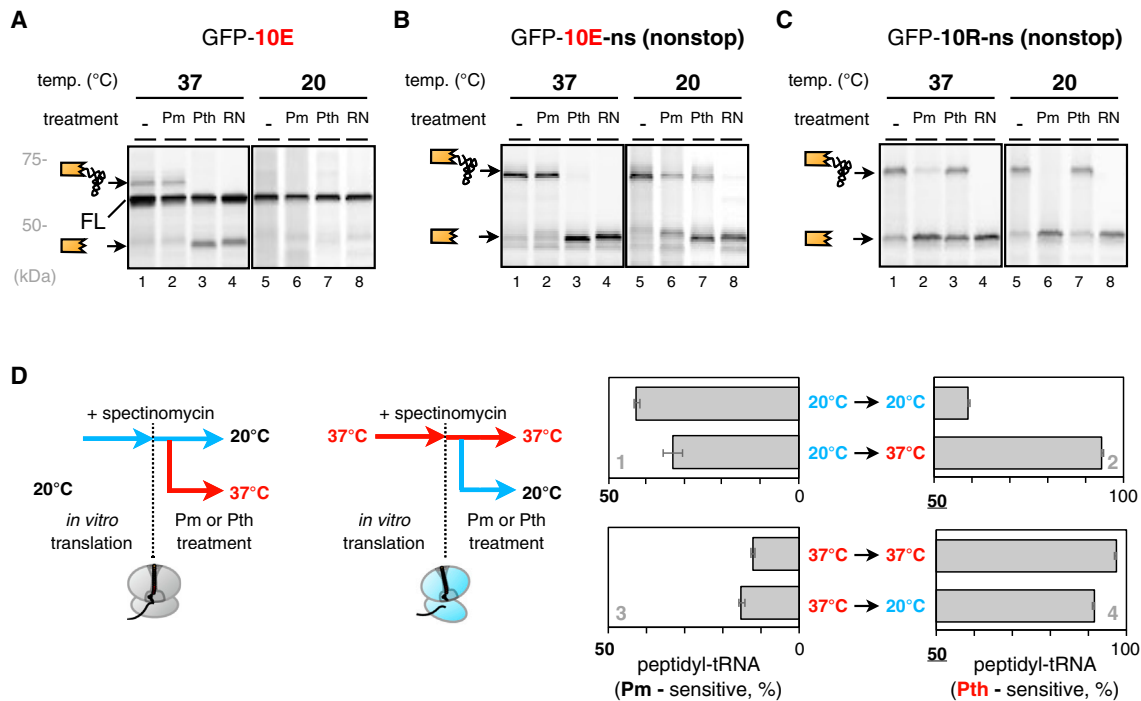
Figure 3. IRD depends on temperature

(A) Repression of IRD at a low temperature. The GFP-10E mRNA was translated by PURE*frex* at 37°C (lanes 1–4) or 20°C (lanes 5–8). Translation products were labeled with Cy5-Met-tRNA. Samples were treated with puromycin (Pm) or peptidyl-tRNA hydrolase (Pth) as indicated and separated by neutral pH SDS-PAGE with an optional RNase A (RN) pretreatment. The position of the full-length polypeptide is indicated by ''FL.'' The peptidyl-tRNA and tRNA-released truncated peptide are schematically indicated.

(B and C) The ribosome resists IRD at a low temperature. The GFP-10E-ns (nonstop, B) or GFP-10R-ns (C) mRNA was translated by PURE*frex* at 37°C (lanes 1–4) or 20°C (lanes 5–8), and the translational products were analyzed as in Figure 3A.

(D) Upper: schematic of the experimental design. The GFP-10E-ns mRNA was translated by PURE*frex* at 20°C (left) or 37°C (right). After the addition of spectinomycin (Figures S3F and S3G) to stop the following elongation reaction, the mixture was treated with puromycin or Pth at 20°C or 37°C. Panels 1 and 2: temperature-dependent stabilization is transient. The proportions of the GFP-10E-ns peptidyl-tRNA translated at 20°C and then shifted from 20°C to 37°C were calculated and plotted. Panels 3 and 4: temperature-dependent destabilization is irreversible. The proportions of GFP-10E-ns peptidyl-tRNA translated at 37°C and that shifted from 37°C to 20°C were calculated and plotted. (#). (#): the mean values ± SE estimated from three independent technical replicates (n = 3) are shown.

indicating that they maintain the basic ribosomal activities (Figure S5A). Taken together with their transient stabilization at low temperatures (Figure 3D), we were prompted to reconstitute the IRD phenomenon using this isolated 70S.

We first examined the temperature-dependent behaviors of IRD in the absence of translation factors. The isolated 70S with GFP-10E-ns was incubated at various temperatures without the addition of translation factors (Figure 5B, left). The occurrence of IRD was evaluated by the Pth-sensitivity of the peptidyl-tRNA. As expected, the stability of the isolated 70S complex varied with temperature (Figure 5C, lanes 1–5). At 4°C (on ice), the Pth resistance of the peptidyl-tRNA persisted, indicating that IRD remained repressed. In contrast, the peptidyl-tRNA accommodated in the isolated 50S subunit was efficiently hydrolyzed by Pth irrespective of temperatures and even at 4°C (Figure S5B). These results suggest that the 70S complex isolated by the SDG fractionation is in a "pre-IRD" state, as we expected.

Unexpectedly, even after incubations at elevated temperatures, the isolated 70S was again stabilized upon the temperature downshift to 4°C, as assessed by the Pth resistance of the

peptidyl-tRNA (Figure 5C, lanes 6–8, schematic in Figure 5B, right). Note that the inclusion of Pth during incubations at higher temperatures produced significant amounts of the peptide fragment (Figure 5C, lanes 3–5). The direct evidence of the "re-stabilization" was provided by the SDG analysis, showing that the isolated 70S almost completely maintained the subunit association even after the incubation at a higher temperature (Figure 5D, from 37°C to 4°C). In addition, the "re-stabilized" 70S was able to catalyze the transpeptidation to puromycin, confirming that the intact PTC structure was maintained (Figure S5C). These results indicate that the temperature-dependent destabilization observed with the isolated 70S complex is reversible.

The reversible stabilization/destabilization of the 70S complex could be attributed to two scenarios: (1) re-association of the dissociated subunits or (2) a conformational rearrangement of the 70S complex without splitting. To distinguish between these possibilities, we depleted the Mg^{2+} in the mixture to definitively split the ribosome complex (Figures 5F, S5D, and S5E). Upon addition of excess Mg^{2+} after Mg^{2+} depletion, the Pth resistance of peptidyl-tRNA never restored irrespective of the amino acids
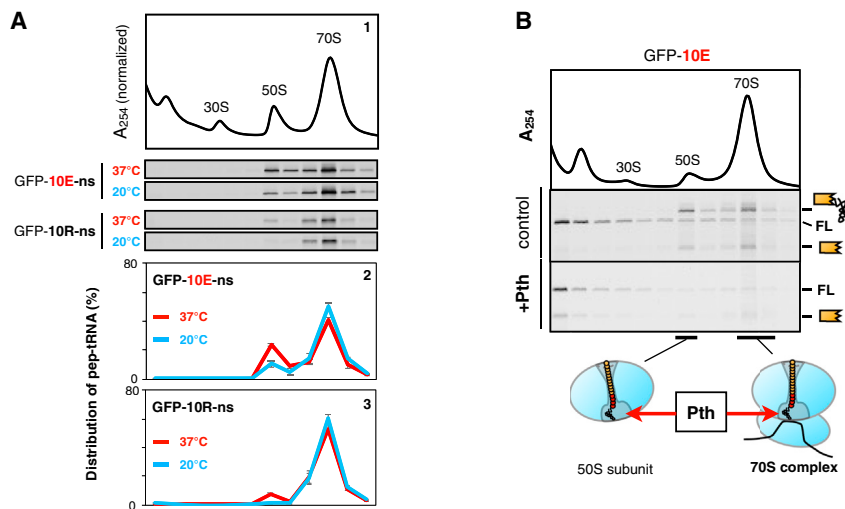
Figure 4. IRD allows Pth to hydrolyze the peptidyl-tRNA within the 70S complex

(A) The GFP-10E-ns or GFP-10R-ns mRNA was translated by PURE*frex* including the ribosomes that were prepared from BL21(*lon ompT*) strain to retain the intact bL31 protein.[64] The Cy5-labeled translational products at the indicated temperatures were fractionated by sucrose density gradient (SDG) ultracentrifugation, separated by SDS-PAGE, and detected by fluorescence. The distribution of the ribosomes was monitored by A_{254} measurement (panel 1). The GFP-10E-ns or GFP-10R-ns peptidyl-tRNAs in each fraction were quantified and plotted in panel 2 or panel 3, respectively (#).

(B) The GFP-10E mRNA was translated by PURE*frex*, including the ribosomes prepared from BL21(*lon ompT*) strain and Cy5-Met-tRNA. The reaction was performed at 37°C, and the resulting mixture was analyzed as shown in Figure 4A. Translation mixture was treated with Pth prior to the SDG ultracentrifugation if indicated. Representatives of two independent experiments were shown. (#): the mean values ± SE estimated from three independent technical replicates (n = 3) are shown.

being accommodated (Figure 5G). This indicates that the dissociated subunits do not readily re-associate (Figure 5H). From these observations, we concluded that the destabilization of the ribosome complex involves a conformational rearrangement rather than subunit splitting.

The destabilized 70S complex is split by ribosome recycling factors

The reversible nature of IRD observed with the isolated 70S complex is superficially inconsistent with the irreversible sensitization of the peptidyl-tRNA to Pth, which we observed in the PURE system reaction at 37°C (Figure 3D). These findings suggested that translation factor(s) may be responsible for the irreversible IRD in the PURE system (Figure 6A). Accordingly, we examined the influence of translation factors on the destabilization of the isolated 70S complex. When Pth was included during the incubation at 37°C, the peptidyl-tRNA ester bond was efficiently hydrolyzed irrespective of the presence or absence of translation factors and cofactors (Figure 6B, upper; Figure 6C, lanes 2 and 3). As already shown, the peptidyl-tRNA in the isolated 70S regained the Pth resistance at 4°C (Figure 6B, lower; Figure 6C, lane 4). However, this reversibility was partially lost in the presence of translation factors (Figure 6C, lane 5), suggesting that a fraction of the ribosome complexes had been destabilized irreversibly. To directly evaluate whether the isolated 70S was split into the subunits, we fractionated the isolated 70S that had been incubated with the translation factors by SDG ultracentrifugation. As expected, the incubation with the translation factors at 37°C split the 70S complex into the subunits (Figure 6D, upper). The co-sedimentation of GFP-10E-ns peptidyl-tRNA with the 50S subunit, in a temperature- and translation factors-dependent manner, provides further evidence for the dissociation of the isolated 70S complex (Figure 6D, lower). Thus, we concluded that the irreversible destabilization represents the splitting of the ribosome complex by the action(s) of translation factor(s).

To identify the translation factor(s) involved in the irreversible dissociation of the pre-IRD 70S complex, we incubated the isolated 70S with each translation factor included in the PURE system, separately and in combination. The temperature-dependent irreversible destabilization was fully reconstituted in the presence of IF3, EF-G, and RRF (Figure 6E). This *in vitro* result was further supported by the facts that the declining concentrations of cellular EF-G and RRF altered the frequency of IRD-dependent translation discontinuation as shown in Figure 1C or in the published ribosome profiling analysis[34] (Figures S6A and S6B). In contrast, RF3, which stimulated the "drop-off" of peptidyl-tRNA,[35–37] had no impact on the IRD (Figure S6C).

Finally, the recycling factors-dependent irreversible splitting was exclusively observed when the isolated 70S accommodates the negatively charged, but not positively charged, nascent chain around the PTC (Figure 6F). Previous studies revealed that IF3, EF-G, and RRF cooperatively split the "post-termination" ribosome complex to recycle the subunits but poorly act on the translating ribosome complex accommodating the peptidyl-tRNA within.[13,14] This difference strongly depends on the presence of the polypeptide part of the peptidyl-tRNA.[13] These imply that the acidic-rich nascent peptide might be considered absent even though it is within the ribosome.

DISCUSSION

The ribosome is a molecular machine that undergoes dynamic conformational rearrangements to catalyze the peptide elongation process. In this study, detailed biochemical analyses unveiled the molecular mechanisms of the IRD-dependent premature termination. First, the occurrence of IRD is associated with the function of EF-G (Figure 1). Second, ribosome stalling significantly increased the frequency of IRD (Figure 2). Third, IRD is greatly affected by temperature (Figure 3). This temperature dependency can be observed in the reconstituted cell-free
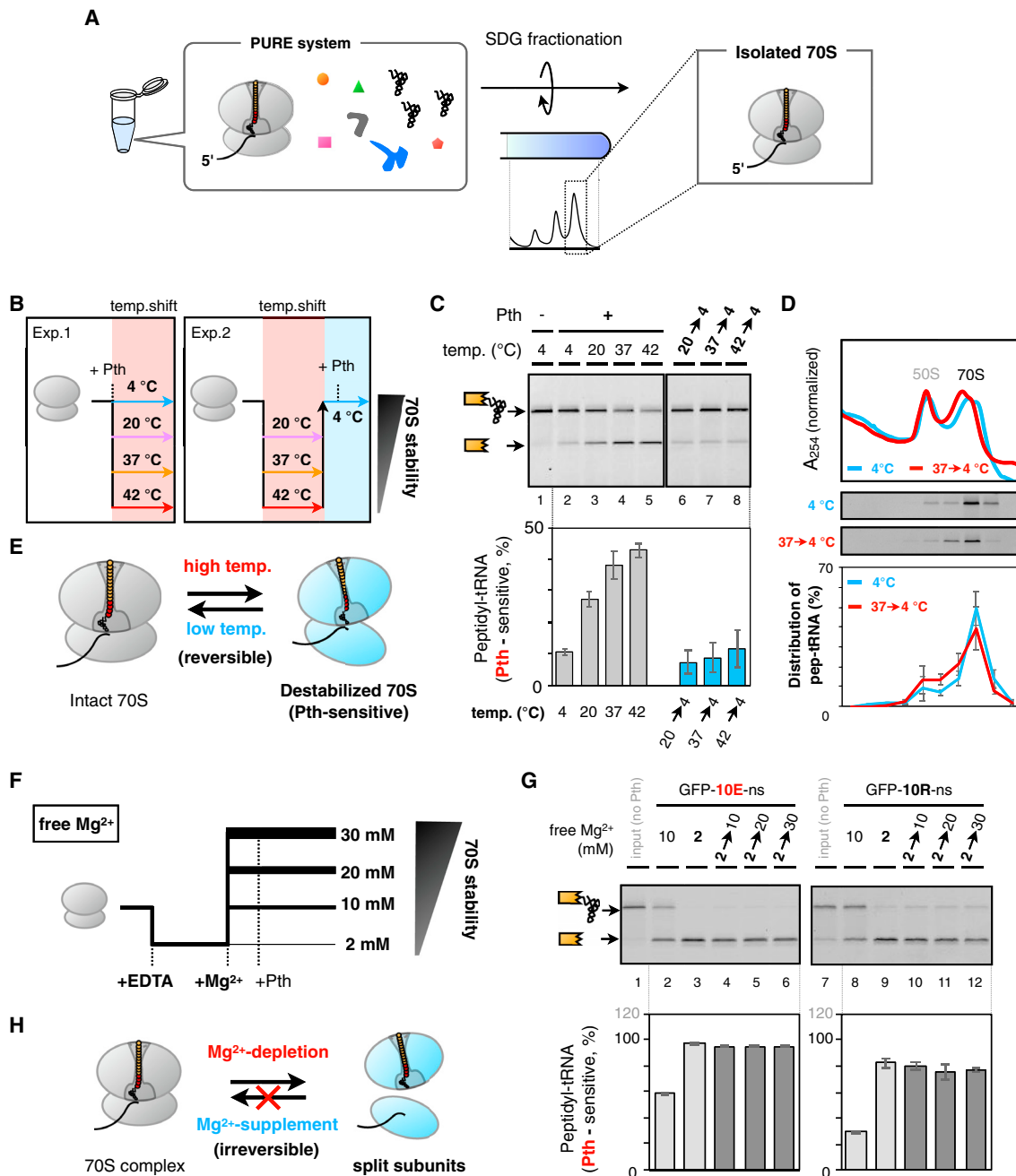
Figure 5. Reversible and spontaneous destabilization of the isolated 70S complex

(A) The 70S ribosome complex accommodating the Cy5-labeled GFP-10E-ns (nonstop) peptidyl-tRNA from the PURE*frex* reaction mixture was isolated by SDG ultracentrifugation.

(B–E) Temperature-dependent reversible destabilization/stabilization of the isolated 70S complex. (B) Schematic of the assay. (C) The isolated 70S of GFP-10E-ns was incubated at the indicated temperatures for 20 min, in the presence (lanes 2–5) or absence (lanes 1, 6, 7, and 8) of Pth. The samples in lanes 6–8 were further incubated on ice (referred to as 4°C) and then treated with Pth for 20 min on ice. The reaction was stopped by TCA precipitation, and samples were separated by neutral pH SDS-PAGE to visualize the Cy5-labeled GFP-10E-ns peptidyl-tRNA and the tRNA-released peptide. The proportion of the GFP-10E-ns peptidyl-tRNA that is Pth cleavable under the indicated conditions was quantified from the gel images and plotted in the lower panel (#). (D) The isolated 70S incubated at 4°C or 37°C was fractionated by SDG ultracentrifugation, separated by SDS-PAGE, and detected by fluorescence. Distributions of the ribosomes were monitored by A_{254} measurement (upper). The GFP-10E nonstop peptidyl-tRNA in each fraction (middle) was quantified and plotted in the lower panel (#). (E) Schematic of the temperature-dependent reversible stabilization/destabilization of the ribosome complex.

(F–H) Irreversible destabilization of the isolated 70S complex by Mg^{2+} depletion. (F) Schematic of the assay. (G) The isolated 70S of GFP-10E-ns (left) or GFP-10R-ns (right) was incubated at 37°C for 20 min in the presence (lanes 2 and 8) or absence (lanes 3–6 and 9–12) of 8 mM EDTA to set the concentration of free Mg^{2+} at

(legend continued on next page)

translation system (Figure 3) and the isolated 70S translating complex (Figures 4, 5, and 6). Fourth, IRD allows Pth to hydrolyze the acidic residue-enriched peptidyl-tRNA within the "70S" ribosome complex (Figures 4 and 5). Finally, IRD allows the splitting of the destabilized 70S ribosome complex triggered by the ribosome recycling pathway without translation termination (Figure 6). Based on these observations, we propose a two-step mechanism for the IRD phenomenon: spontaneous structural alternation of the 70S ribosome followed by subsequent subunit splitting (Figure 7).

The unveiled features of IRD in the isolated "pre-IRD" 70S are temperature dependence, reversibility, and the occurrence independent of translation factors (Figure 6). Similar characteristics of the ribosome have also been reported in the ratchet-like rotation observed in structural studies by time-resolved cryo-EM[1] and single-molecule FRET analyses.[2] The ratcheting motion is considered a driving force to translocate the peptidyl-tRNA in the A-site after transpeptidation.[1] However, Frank and colleagues reported that the ratchet-like rotation is "locked" when the peptidyl-tRNA is located within the P-site,[3] because the futile rotation could trigger translational errors.[4] Furthermore, the "lock" of the rotation depends on the nascent polypeptide within the tunnel.[2,3] The behavior of the destabilized ribosome as if it does not accommodate the nascent peptide could be indicative of an impairment in the "lock" function of the peptidyl-tRNA molecule. Recent molecular simulations by O'Brien and colleagues indicated the possibility that the negatively charged nascent chain pulls itself from the P-site to the A-site, resulting in a position shift.[38] Such aberrant localization of the peptidyl-tRNA could weaken the ribosome-tRNA interactions. Related to this speculation, it is worth noting that the deacylated tRNA located within the P-site can adopt a P/E hybrid state.[3,39,40] This aligns with the "locking" hypothesis and the observation that RRF, responsible for dissociating the pre-IRD complex, associates with the 70S ribosomes accommodating a tRNA in the P/E hybrid state.[41,42] To prove these assumptions, further analyses, including structural observations in the future, are required.

Translation of the IRD sequence allows the ribosome recycling pathway to split the associated subunits (Figure 6). Previous studies have shown that recycling factors originally split the post-termination complex that carries the deacylated tRNA within the P-site but not the ribosome containing the growing peptidyl-tRNA.[13,15,43] This feature is reasonable to avoid futile premature termination and is consistent with our hypothesis that nascent peptide "disappears" during the translation of the IRD sequence, as discussed above. EF-G interacts with and stabilizes the ribosome complex in the hybrid state but less so in the classic state.[3,26,44–49] RRF fixes the post-termination complex in the hybrid state to prepare the subsequent EF-G-catalyzed splitting.[41,42,50] From these observations, the recycling factors would not act in concert with temperature-dependent structural rearrangements but instead split the destabilized ribosome complex after it has been structurally rearranged (Figure 7).

It is noteworthy that the peptidyl-tRNA hydrolysis ultimately depends on Pth, regardless of the subunit splitting. This means that Pth acts as a noncanonical release factor for the destabilized ribosome complex. On a related note, Varshney and colleagues found that the lethality of the pth^{ts} mutant at a nonpermissive temperature is suppressed by the decreased activities of RRF and IF3.[14] This suggests that E. coli can grow even if the Pth activity is reduced, as long as the amounts of Pth substrates, including IRD-derived peptidyl-tRNAs, are reduced due to the compromised activity of the recycling pathway. This also implies that the destabilized 70S ribosome, which is suspended on the mRNA, could stochastically resume the translation elongation.

Pth is basically unable to access the peptidyl-tRNA within the intact 70S complex,[51,52] implying that the conformation of the 70S complex is somehow altered. In our previous study using the bL31-truncated ribosome, we observed a complete dissociation of the destabilized 70S complex, which would enable Pth to hydrolyze the peptidyl-tRNA.[21] However, in our current study, we found that most of the IRD-prone peptidyl-tRNA is associated with the 70S complex and can be cleaved by Pth without the subunit dissociation. The C-terminal truncation of bL31 had a limited impact on the frequency of IRD but influenced the results of SDG ultracentrifugation analysis (Figure S4). Based on these observations, we would like to revise our consideration that bacterial IRD does not necessarily involve splitting of the 70S complex,[21] as well as the eukaryotic ribosome.[23]

We have already shown that the intrinsically destabilized eukaryotic ribosome allows the Pth2p-mediated hydrolysis of peptidyl-tRNA without subunit dissociation.[23] Since the PTC structure and the mechanism of elongation are common to both eukaryotes and prokaryotes, we assume that the basic mechanism of IRD is also common. The ester bond of peptidyl-tRNA is shielded by the PTC architecture, thereby preventing access and cleavage by Pth. We, therefore, speculate that the nascent peptide protrudes or is partly ejected from the tunnel through a mechanism involving negative-negative repulsion.

Ribosome stalling increased the frequency of IRD (Figure 2). Prolonged stalling would provide more chances for conformational rearrangements or premature recycling if the IRD sequence is within the ribosome. If the elongation steadily proceeds, such events should be competitively avoided by the accommodation of an aminoacyl-tRNA and the following transpeptidation (Figure 2A). In physiological situations, various environmental stresses such as starvation, oxidative stress, and UV irradiation inhibit translation elongation.[53–55] The IRD-dependent regulations, such as mgtL-mgtA[21] or N-terminal DE/P-enriched sequences,[22] may also become more significant during stress conditions. In another perspective, IRD sequences could potentially act as alternative "translation termination signals" to quickly interrupt protein synthesis. In our ribosome profiling analyses conducted under the nutrient-rich condition, we have estimated that approximately 15% of ribosomes undergo premature termination during the translation of N-terminal acidic residue-rich
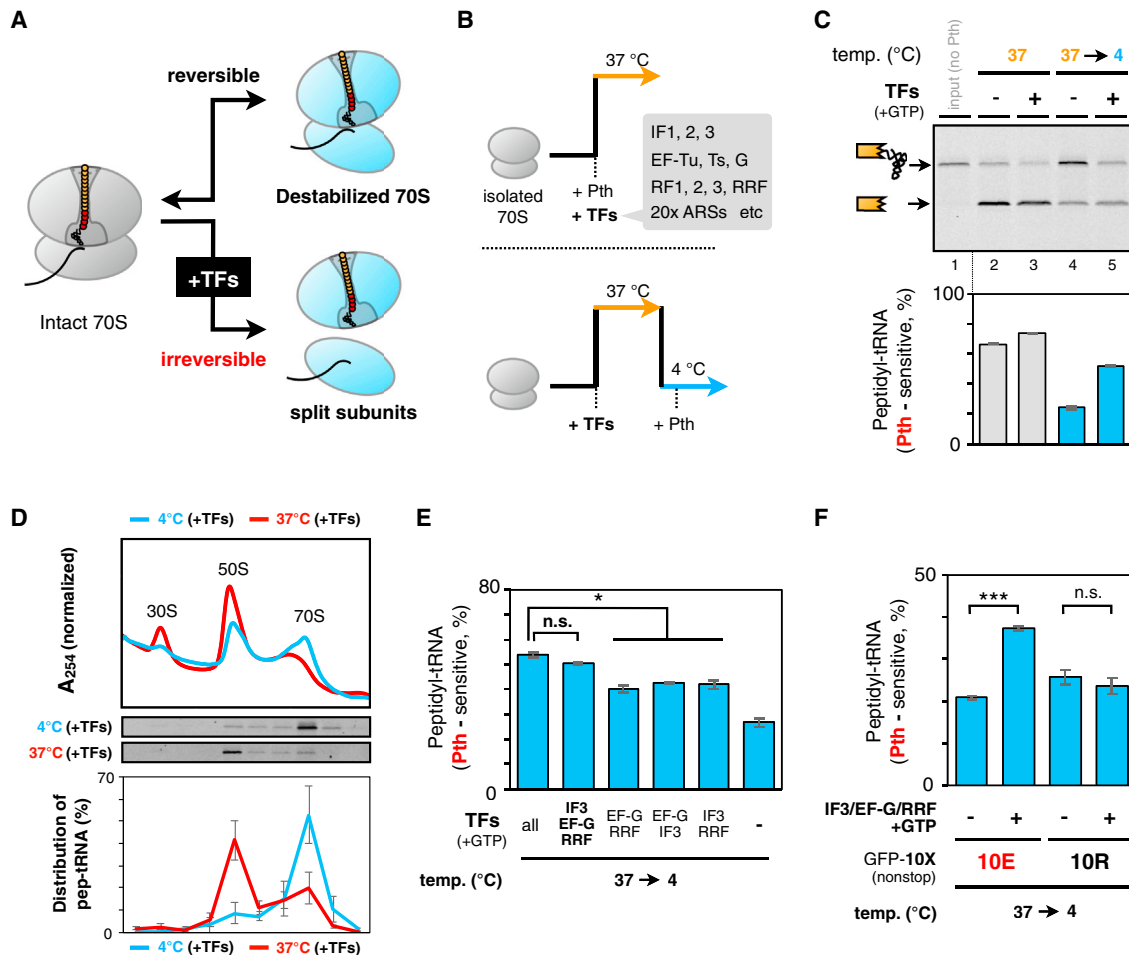
Figure 6. IRD allows the futile splitting by ribosome recycling factors

(A–D) Translation factors irreversibly split the destabilized 70S complex. (A) Working hypothesis: a translation factor(s) is the determinant for the reversibility/irreversibility of the destabilization. (B) Schematic of the assay. (C) The isolated 70S was incubated at 37°C in the presence (lanes 3 and 5) or absence (lanes 2 and 4) of translation factors included in the PUREfrex system. The 70S was treated with Pth during the 37°C incubation (lanes 2 and 3) or after standing on ice for re-stabilization (4°C, lanes 4 and 5). The proportion of GFP-10E-ns peptidyl-tRNA that can be cleaved by Pth was quantified from the gel images and plotted in the lower panel (#). (D) The isolated 70S incubated at 4°C or 37°C in the presence or absence of translation factors was fractionated by SDG ultracentrifugation, separated by SDS-PAGE, and detected by fluorescence. Distributions of the ribosomes were monitored by A_{254} measurement (upper). The GFP-10E-ns peptidyl-tRNAs in each fraction (middle) were quantified and plotted in the lower panel (#).

(E) IF3, EF-G, and RRF cooperatively split the destabilized ribosome. The isolated 70S was incubated at 37°C in the presence of translation factors and 1 mM GTP as indicated and then placed on ice and further incubated with Pth, as in Figure 6C. *p value < 0.05; n.s., no significant difference (Welch's t test) (#).

(F) Recycling factors exclusively split the destabilized ribosome but not the translating ribosome. The isolated 70S of GFP-10E-ns or GFP-10R-ns was incubated in the presence or absence of IF3, EF-G, and RRF at 37°C in the presence of 1 mM GTP and then placed on ice and treated with Pth as described above. ***p value <0.001; n.s., no significant difference (Welch's t test) (#). (#): the mean values ± SE estimated from three independent technical replicates (n = 3) are shown.

sequences.[22] This could be even more pronounced under stress conditions, such as nutrient depletion, potentially leading to a bias in proteome expression. Alternatively, IRD might generate alternative protein isoforms through premature termination under stress conditions. From this perspective, it is worth noting that aspartic acid and glutamic acid were utilized for peptide synthesis in an early stage of evolution.[56] IRD might have served as a means of translation termination in the primitive translation system.

Numerous studies have shown that the nascent peptide variously and dynamically regulates translation elongation. Our recent and present studies also demonstrate that nascent peptides could dictate the stability of the ribosome complex.[21–23] The stability of the ribosome complex is positively and negatively influenced by various environmental factors, including metal ions such as K^+ and Mg^{2+},[16,19,57] polyamines,[58] and temperature.[17–20] These imply that nascent peptide-dependent regulations, including IRD, could be utilized in a variety of situations beyond our current understanding. We believe that the data presented here have revealed a part of the behind-the-scenes details of the translation dynamics and provide clues to expose "hidden" genetic codes of various organisms.
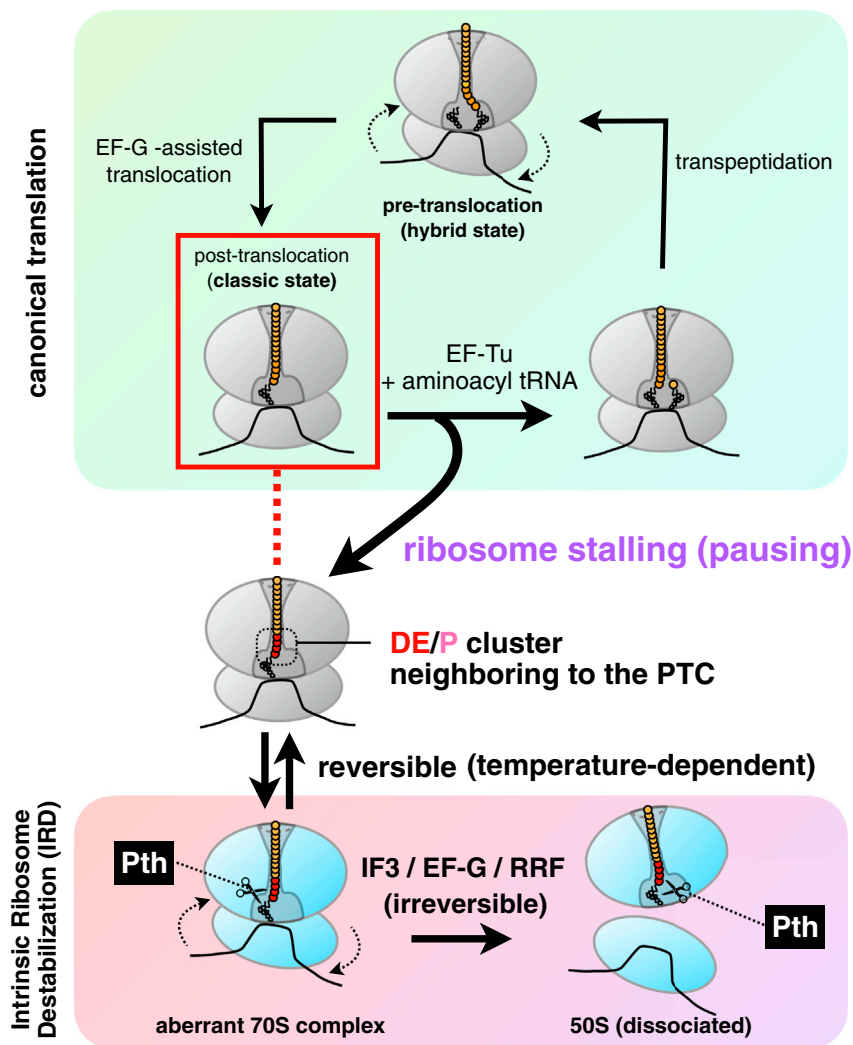
Figure 7. Model: a two-step mechanism for the IRD phenomenon

The flow of the IRD phenomenon, as elucidated by this study. When the ribosome is in the classic state (Figure 2), the accommodated nascent peptide enriched with acidic residues could trigger the structural rearrangement of the 70S complex in a temperature-dependent manner (Figure 3). This structural alternation is reversible and independent of translation factors (Figure 5). The resulting structural rearrangement allows Pth-induced hydrolysis of the peptidyl-tRNA without subunit splitting (Figures 4 and 5). In parallel, ribosome recycling factors (IF3, EF-G, and RRF) split this "70S" ribosome complex in an aberrant state for the premature translation termination (Figures 1 and 6).

Limitations of the study

We have conducted a detailed investigation into the molecular mechanisms of nascent peptide-induced IRD. However, it is important to note that our data do not provide direct evidence of the conformational rearrangement of the destabilized 70S ribosome complex. Additionally, we have yet to elucidate the molecular detail of how Pth cleaves the peptidyl-tRNAs that are associated with the destabilized 70S complex. Addressing these questions will necessitate further in-depth analysis, potentially involving a structural observation of the destabilized ribosome complex or an application of single-molecule techniques capable of discerning the rotation state of the ribosome complex.

STAR★METHODS

Detailed methods are provided in the online version of this paper and include the following:

- KEY RESOURCES TABLE
- RESOURCE AVAILABILITY
  - ○ Lead contact
  - ○ Materials availability
  - ○ Data and code availability
- EXPERIMENTAL MODEL AND STUDY PARTICIPANT DETAILS
  - ○ Bacterial strains
  - ○ Growth conditions
- METHOD DETAILS
  - ○ *E. coli* strains, plasmids, and primers
  - ○ *In vitro* translation and product analysis
  - ○ β-galactosidase assay
  - ○ TC index (*in vivo*) = $m.u.(DE/P^+)/m.u.(no\ DEP)$
  - ○ IRD reconstitution using the isolated 70S complex
  - ○ Ribo-seq analysis
- QUANTIFICATION AND STATISTICAL ANALYSIS
  - ○ Statistical analyses
  - ○ Quantification of the signals from gel images
  - ○ Proportions of peptidyl-tRNAs that are sensitive to puromycin/Pth
  - ○ Distribution of pep-tRNA in the SDG analysis

AUTHOR CONTRIBUTIONS

Y.C. performed experiments; T.K. prepared the purified components for *in vitro* translation; K.I. analyzed the published ribosome profiling dataset; Y.C. designed experiments and analyzed the results; Y.C., T.K., T.N., K.I., K.I.N., A.M., and H.T. conceived the study; Y.C. and H.T. supervised the entire project and wrote the manuscript.

DECLARATION OF INTERESTS

The authors declare no competing interests.

REFERENCES

1. Fischer, N., Konevega, A.L., Wintermeyer, W., Rodnina, M.V., and Stark, H. (2010). Ribosome dynamics and tRNA movement by time-resolved electron cryomicroscopy. Nature *466*, 329–333.

2. Cornish, P.V., Ermolenko, D.N., Noller, H.F., and Ha, T. (2008). Spontaneous Intersubunit Rotation in Single Ribosomes. Mol. Cell *30*, 578–588.

3. Valle, M., Zavialov, A., Sengupta, J., Rawat, U., Ehrenberg, M., and Frank, J. (2003). Locking and Unlocking of Ribosomal Motions. Cell *114*, 123–134.

4. Zhou, J., Lancaster, L., Donohue, J.P., and Noller, H.F. (2019). Spontaneous ribosomal translocation of mRNA and tRNAs into a chimeric hybrid state. Proc. Natl. Acad. Sci. USA *116*, 7813–7818.

5. Ito, K., and Chiba, S. (2013). Arrest Peptides: Cis-Acting Modulators of Translation. Annu. Rev. Biochem. *82*, 171–202.

6. Schlessinger, D., Mangiarotti, G., and Apirion, D. (1967). The formation and stabilization of 30S and 50S ribosome couples in *Escherichia coli*. Proc. Natl. Acad. Sci. USA *58*, 1782–1789.

7. Kohler, R.E., Ron, E.Z., and Davis, B.D. (1968). Significance of the free 70 s ribosomes in *Escherichia coli* extracts. J. Mol. Biol. *36*, 71–82.

8. Ron, E.Z., Kohler, R.E., and Davis, B.D. (1968). Magnesium ion dependence of free and polysomal ribosomes from *Escherichia coli*. J. Mol. Biol. *36*, 83–89.

9. van Duin, J., VAN Dieijen, G., Dieijen, G., van Knippenberg, P.H., and Bosch, L. (1970). Different Species of 70S Ribosomes of *Escherichia coli* and their Dissociation into Subunits. Eur. J. Biochem. *17*, 433–440.

10. Ali, I.K., Lancaster, L., Feinberg, J., Joseph, S., and Noller, H.F. (2006). Deletion of a Conserved, Central Ribosomal Intersubunit RNA Bridge. Mol. Cell *23*, 865–874.

11. Zylber, E.A., and Penman, S. (1970). The effect of high ionic strength on monomers, polyribosomes, and puromycin-treated polyribosomes. Biochim. Biophys. Acta *204*, 221–229.

12. Blobel, G., and Sabatini, D. (1971). Dissociation of Mammalian Polyribosomes into Subunits by Puromycin. Proc. Natl. Acad. Sci. USA *68*, 390–394.

13. Peske, F., Rodnina, M.V., and Wintermeyer, W. (2005). Sequence of Steps in Ribosome Recycling as Defined by Kinetic Analysis. Mol. Cell *18*, 403–412.

14. Singh, N.S., Das, G., Seshadri, A., Sangeetha, R., and Varshney, U. (2005). Evidence for a role of initiation factor 3 in recycling of ribosomal complexes stalled on mRNAs in *Escherichia coli*. Nucleic Acids Res. *33*, 5591–5601.

15. Zavialov, A.V., Hauryliuk, V.V., and Ehrenberg, M. (2005). Splitting of the Posttermination Ribosome into Subunits by the Concerted Action of RRF and EF-G. Mol. Cell *18*, 675–686.

16. Tissières, A., Watson, J.D., Schlessinger, D., and Hollingworth, B.R. (1959). Ribonucleoprotein particles from. Escherichia coli *1*, 221–233.

17. Hamburger, A.D., LAPIDOT, Y., and De Groot, N. (1973). Thermal Stability of Poly(U) · tRNA: Ribosome Complexes with Phe-tRNA^Phe and Peptidyl-tRNA^Phe. Eur. J. Biochem. *32*, 576–583.

18. Korber, P., Stahl, J.M., Nierhaus, K.H., and Bardwell, J.C. (2000). Hsp15: a ribosome-associated heat shock protein. EMBO J. *19*, 741–748.

19. Zitomer, R.S., and Flaks, J.G. (1972). Magnesium dependence and equilibrium of the *Escherichia coli* ribosomal subunit association. J. Mol. Biol. *71*, 263–279.

20. Safdari, H.A., Kasvandik, S., Polte, C., Ignatova, Z., Tenson, T., and Wilson, D.N. (2022). Structure of *Escherichia coli* heat shock protein Hsp15 in complex with the ribosomal 50S subunit bearing peptidyl-tRNA. Nucleic Acids Res. *50*, 12515–12526.

21. Chadani, Y., Niwa, T., Izumi, T., Sugata, N., Nagao, A., Suzuki, T., Chiba, S., Ito, K., and Taguchi, H. (2017). Intrinsic Ribosome Destabilization Underlies Translation and Provides an Organism with a Strategy of Environmental Sensing. Mol. Cell *68*, 528–539.e5.

22. Chadani, Y., Sugata, N., Niwa, T., Ito, Y., Iwasaki, S., and Taguchi, H. (2021). Nascent polypeptide within the exit tunnel stabilizes the ribosome to counteract risky translation. EMBO J. *40*, e108299.

23. Ito, Y., Chadani, Y., Niwa, T., Yamakawa, A., Machida, K., Imataka, H., and Taguchi, H. (2022). Nascent peptide-induced translation discontinuation in eukaryotes impacts biased amino acid usage in proteomes. Nat. Commun. *13*, 7451.

24. Rodnina, M.V. (2018). Translation in Prokaryotes. CSH. Perspect. Biol. *10*, a032664.

25. Rodnina, M.V., Savelsbergh, A., Katunin, V.I., and Wintermeyer, W. (1997). Hydrolysis of GTP by elongation factor G drives tRNA movement on the ribosome. Nature *385*, 37–41.

26. Liu, G., Song, G., Zhang, D., Zhang, D., Li, Z., Lyu, Z., Dong, J., Achenbach, J., Gong, W., Zhao, X.S., et al. (2014). EF-G catalyzes tRNA translocation by disrupting interactions between decoding center and codon-anticodon duplex. Nat. Struct. Mol. Biol. *21*, 817–824.

27. Hou, Y., Lin, Y.P., Sharer, J.D., and March, P.E. (1994). In vivo selection of conditional-lethal mutations in the gene encoding elongation factor G of *Escherichia coli*. J. Bacteriol. *176*, 123–129.

28. Müller, C., Crowe-McAuliffe, C., and Wilson, D.N. (2021). Ribosome Rescue Pathways in Bacteria. Front. Microbiol. *12*, 652980.

29. Chadani, Y., Ono, K., Ozawa, S.I., Takahashi, Y., Takai, K., Nanamiya, H., TOZAWA, Y., Kutsukake, K., and Abo, T. (2010). Ribosome rescue by *Escherichia coli* ArfA (YhdL) in the absence of *trans*-translation system. Mol. Microbiol. *78*, 796–808.

30. Chadani, Y., Ono, K., Kutsukake, K., and Abo, T. (2011). *Escherichia coli* YaeJ protein mediates a novel ribosome-rescue pathway distinct from SsrA- and ArfA-mediated pathways. Mol. Microbiol. *80*, 772–785.

31. Chadani, Y., Ito, K., Kutsukake, K., and Abo, T. (2012). ArfA recruits release factor 2 to rescue stalled ribosomes by peptidyl-tRNA hydrolysis in *Escherichia coli*. Mol. Microbiol. *86*, 37–50.

32. Handa, Y., Inaho, N., and Nameki, N. (2011). YaeJ is a novel ribosome-associated protein in *Escherichia coli* that can hydrolyze peptidyl–tRNA on stalled ribosomes. Nucleic Acids Res. *39*, 1739–1748.

33. Shimizu, Y. (2012). ArfA Recruits RF2 into Stalled Ribosomes. J. Mol. Biol. *423*, 624–631.

34. Saito, K., Green, R., and Buskirk, A.R. (2020). Ribosome recycling is not critical for translational coupling in *Escherichia coli*. Elife *9*, e59974.

35. Heurgué-Hamard, V., Karimi, R., Mora, L., MacDougall, J., Leboeuf, C., Grentzmann, G., Ehrenberg, M., and Buckingham, R.H. (1998). Ribosome release factor RF4 and termination factor RF3 are involved in dissociation of peptidyl-tRNA from the ribosome. EMBO J. *17*, 808–816.

36. Dinçbas, V., Heurgué-Hamard, V., Buckingham, R.H., Karimi, R., and Ehrenberg, M. (1999). Shutdown in protein synthesis due to the expression of mini-genes in bacteria. J. Mol. Biol. *291*, 745–759.

37. Nagao, A., Nakanishi, Y., Yamaguchi, Y., Mishina, Y., Karoji, M., Toya, T., Fujita, T., Iwasaki, S., Miyauchi, K., Sakaguchi, Y., and Suzuki, T. (2023). Quality control of protein synthesis in the early elongation stage. Nat. Commun. *14*, 2704.

38. Leininger, S.E., Rodriguez, J., Vu, Q.V., Jiang, Y., Li, M.S., Deutsch, C., and O'Brien, E.P. (2021). Ribosome Elongation Kinetics of Consecutively Charged Residues Are Coupled to Electrostatic Force. Biochemistry-us *60*, 3223–3235.

39. Agrawal, R.K., Penczek, P., Grassucci, R.A., Burkhardt, N., Nierhaus, K.H., and Frank, J. (1999). Effect of Buffer Conditions on the Position of tRNA on the 70 S Ribosome As Visualized by Cryoelectron Microscopy*. J. Biol. Chem. *274*, 8723–8729.

40. McGarry, K.G., Walker, S.E., Wang, H., and Fredrick, K. (2005). Destabilization of the P Site Codon-Anticodon Helix Results from Movement of tRNA into the P/E Hybrid State within the Ribosome. Mol. Cell *20*, 613–622.

41. Prabhakar, A., Capece, M.C., Petrov, A., Choi, J., and Puglisi, J.D. (2017). Post-termination Ribosome Intermediate Acts as the Gateway to Ribosome Recycling. Cell Rep. *20*, 161–172.

42. Dunkle, J.A., Wang, L., Feldman, M.B., Pulk, A., Chen, V.B., Kapral, G.J., Noeske, J., Richardson, J.S., Blanchard, S.C., and Cate, J.H.D. (2011). Structures of the Bacterial Ribosome in Classical and Hybrid States of tRNA Binding. Science *332*, 981–984.

43. Hirokawa, G., Nijman, R.M., RAJ, V.S., Kaji, H., Igarashi, K., and Kaji, A. (2005). The role of ribosome recycling factor in dissociation of 70S ribosomes into subunits. RNA *11*, 1317–1328.

44. Zavialov, A.V., and Ehrenberg, M. (2003). Peptidyl-tRNA Regulates the GTPase Activity of Translation Factors. Cell *114*, 113–122.

45. Frank, J., and Agrawal, R.K. (2000). A ratchet-like inter-subunit reorganization of the ribosome during translocation. Nature *406*, 318–322.

46. Tourigny, D.S., Fernández, I.S., Kelley, A.C., and Ramakrishnan, V. (2013). Elongation Factor G Bound to the Ribosome in an Intermediate State of Translocation. Science *340*, 1235490.

47. Zhou, J., Lancaster, L., Donohue, J.P., and Noller, H.F. (2013). Crystal Structures of EF-G–Ribosome Complexes Trapped in Intermediate States of Translocation. Science *340*, 1236086.

48. Pulk, A., and Cate, J.H.D. (2013). Control of Ribosomal Subunit Rotation by Elongation Factor G. Science *340*, 1235970.

49. Spiegel, P.C., Ermolenko, D.N., and Noller, H.F. (2007). Elongation factor G stabilizes the hybrid-state conformation of the 70S ribosome. RNA *13*, 1473–1482.

50. Borg, A., Pavlov, M., and Ehrenberg, M. (2016). Complete kinetic mechanism for recycling of the bacterial ribosome. RNA *22*, 10–21.

51. de Groot, N., Panet, A., and Lapidot, Y. (1968). Enzymatic hydrolysis of peptidyl-tRNA. Biochem. Biophys. Res. Commun. *31*, 37–42.

52. Menninger, J.R., Mulholland, M.C., and Stirewalt, W.S. (1970). Peptidyl-tRNA hydrolase and protein chain termination. Biochim. Biophys. Acta *217*, 496–511.

53. Wu, C.C.-C., Peterson, A., Zinshteyn, B., Regot, S., and Green, R. (2020). Ribosome Collisions Trigger General Stress Responses to Regulate Cell Fate. Cell *182*, 404–416.e14.

54. Simms, C.L., Hudson, B.H., Mosior, J.W., Rangwala, A.S., and Zaher, H.S. (2014). An Active Role for the Ribosome in Determining the Fate of Oxidized mRNA. Cell Rep. *9*, 1256–1264.

55. Li, X., Yagi, M., Morita, T., and Aiba, H. (2008). Cleavage of mRNAs and role of tmRNA system under amino acid starvation in *Escherichia coli*. Mol. Microbiol. *68*, 462–473.

56. Miller, S.L. (1953). A Production of Amino Acids Under Possible Primitive Earth Conditions. Science *117*, 528–529.

57. Nierhaus, K.H. (2014). Mg^{2+}, K^+, and the Ribosome. J. Bacteriol. *196*, 3817–3819.

58. Cohen, S.S., and Lichtenstein, J. (1960). Polyamines and Ribosome Structure. J. Biol. Chem. *235*, 2112–2116.

59. Baba, T., Ara, T., Hasegawa, M., Takai, Y., Okumura, Y., Baba, M., Datsenko, K.A., Tomita, M., Wanner, B.L., and Mori, H. (2006). Construction of *Escherichia coli* K-12 in-frame, single-gene knockout mutants: the Keio collection. Mol. Syst. Biol. *2*, 2006.0008.

60. Datsenko, K.A., and Wanner, B.L. (2000). One-step inactivation of chromosomal genes in *Escherichia coli* K-12 using PCR products. Proc. Natl. Acad. Sci. USA *97*, 6640–6645.

61. Ohashi, H., Shimizu, Y., Ying, B.-W., and Ueda, T. (2007). Efficient protein selection based on ribosome display system with purified components. Biochem. Biophys. Res. Commun. *352*, 270–276.

62. Shimizu, Y., Inoue, A., Tomari, Y., Suzuki, T., Yokogawa, T., Nishikawa, K., and Ueda, T. (2001). Cell-free translation reconstituted with purified components. Nat. Biotechnol. *19*, 751–755.

63. Ichihara, K., Matsumoto, A., Nishida, H., Kito, Y., Shimizu, H., Shichino, Y., Iwasaki, S., Imami, K., Ishihama, Y., and Nakayama, K.I. (2021). Combinatorial analysis of translation dynamics reveals eIF2 dependence of translation initiation at near-cognate codons. Nucleic Acids Res. *49*, 7298–7317.

64. Ueta, M., Wada, C., Bessho, Y., Maeda, M., and Wada, A. (2017). Ribosomal protein L31 in *Escherichia coli* contributes to ribosome subunit association and translation, whereas short L31 cleaved by protease 7 reduces both activities. Gene Cell. *22*, 452–471.

Cell Reports
Article

STAR★METHODS

KEY RESOURCES TABLE

REAGENT or RESOURCE	SOURCE	IDENTIFIER
Bacterial and virus strains		
BW25113	Laboratory stock	CGSC7636
BL21(DE3)	Laboratory stock	CGSC12504
A19	Laboratory stock	CGSC5997
Strains used in this study derived from BW25113 are listed in Table S1.	This study	N/A
P1 bacteriophage	Laboratory stock	CGSC12133
Chemicals, peptides, and recombinant proteins		
Easy tag L-[35S]-Methionine	PerkinElmer	NEG709A005MC
WIDE RANGE Gel Preparation Buffer (4X) for PAGE	nacalai tesque	07831–94
RNase A Solution, 4 mg/ml	Promega	A7973
Cy5 NHS Ester Mono-reactive Dye Pack	GE healthcare	PA25001
ONPG	WAKO	146–04694
Critical commercial assays		
PUREfrex 1.0	GeneFrontier	PF001
Deposited data		
Mendeley Database	This study	https://doi.org/10.17632/3bbnxh366s.1
Ribosome profiling data reanalyzed in this study	Saito et al., 2020[34] (https://doi.org/10.7554/eLife.59974)	GSE151688
Oligonucleotides		
Oligonucleotide used in this study are listed in Table S3.	This study	N/A
Recombinant DNA		
Plasmids used in this study are listed in Table S2.	This study	N/A
Software and algorithms		
Microsoft Excel	Microsoft	N/A
R	R project	www.r-project.org
FLA7000 image analyzer	Fujifilm/GE healthcare	N/A
Scanner Control Software	Cytiva	N/A
Multi Gauge	Fujifilm/GE healthcare	N/A
Custom Python script	Ichihara et al., 2021[63]	https://doi.org/10.1093/nar/gkab549

RESOURCE AVAILABILITY

Lead contact
Please direct any requests for further information or reagents to the lead contact, Yuhei Chadani (ychadani@okayama-u.ac.jp).

Materials availability
Bacterial strains and plasmids are available upon request (MTA completion required).

Data and code availability
- Unprocessed data and plasmid sequences used in this study are available in the Mendeley repository (https://doi.org/10.17632/3bbnxh366s.1).
- This study does not report original code.
- All data reported in this paper will be shared by the lead contact upon request.

EXPERIMENTAL MODEL AND STUDY PARTICIPANT DETAILS

Bacterial strains

BW25113 {Δ(*araD-araB*)567, Δ*lacZ4787*(:*rrnB*-3), λ-, *rph*-1, Δ(*rhaD-rhaB*)568, *hsdR514*}, a derivative of *Escherichia coli* K-12 was used as the experimental standard strain. Other bacterial strains, and plasmids used in this study are listed in Tables S1 and S2, respectively. Construction schemes were provided in METHODS DETAILS.

Growth conditions

E. coli cells harboring the reporter plasmid were grown overnight at 37°C in LB medium supplemented with 100 μg/mL of ampicillin. They were diluted 1:500 into fresh LB supplemented with ampicillin and 2x 10^{-4}% arabinose. The cultures were allowed to grow at 37°C for approximately 2.5 h (A_{660} = ~0.2). Subsequently, the temperature was shifted to 42°C if indicated, and growth continued until the A_{660} doubled.

METHOD DETAILS

E. coli strains, plasmids, and primers

E. coli strains, plasmids, and oligonucleotides used in this study are listed in Tables S1, S2, and S3, respectively. The KEIO collection library[59] was obtained from the National BioResource Project (NBRP). Plasmids were constructed using standard cloning procedures and Gibson assembly. Detailed schemes are summarized in Table S2, and sequences of constructed plasmids are available in the Mendeley repository (https://doi.org/10.17632/3bbnxh366s.1).

The PCR-amplified DNA fragment from pTGT1 (Tet[R]), obtained using the primers PT0912 (CAGACTTACGGTTAAGCACCCCAG CCAGATGGCCTGGTGAATTCCGGGGATCCGTCGACC) and PT0913 (ATTTTAAAAACAGAAACATTCATATTTAAAATGTTAAATTG TGTAGGCTGGAGCTGCTTC), was further amplified by a second PCR, using PT0914 (CTGATTTCGTCAGACTTACGGTTAA GCAC) and PT0915 (CAAATGAAGCATTTTAAAAACAGAAACATTC). The purified DNA fragment was electroporated into strain BW25113 harboring pKD46[60] and pCY3395 (*rpsL-rpsG-fusA-tufA* operon), with selections for a tetracycline (10 μg/mL) and specti-nomycin (100 μg/mL)-resistant transformant, to obtain ECY0725. The genome-introduced Δ*rpsJ-rpsQ*::FRT-Tet[R]-FRT mutation was transferred by phage P1 into BW25113 harboring pCY3395 (*rpsL-rpsG-fusA-tufA* operon) or pCY3401 (*rpsL-rpsG-fusA-tufA* operon carrying *fusA* G502D mutation) to obtain ECY0726 and ECY0729, respectively.

In vitro translation and product analysis

The coupled transcription-translation reaction was performed using PURE*frex 1.0* (GeneFrontier) in the presence of ^{35}S-methionine or Cy5-Met-tRNA[fMet] at the indicated temperature (for 30 min at 37°C or for 60 min at 30, 24, 20°C). N-terminal fluorescent labeling of PURE*frex* translation products was performed using pre-charged Cy5-Met-tRNA, as described previously.[21] In detail, tRNA[fMet] was overexpressed in strain BL21 (DE3) carrying pGEMEX-tRNA[fMet]. Cells were harvested and lysed by vigorous shaking with acidic phenol-0.3 M potassium acetate solution. The aqueous phase was collected and RNA molecules were precipitated with ethanol, dis-solved in 50 mM sodium carbonate buffer (pH 9.1), and back-extracted with acidic phenol and ethanol-precipitated again. tRNA[fMet] was purified by anion exchange chromatography with elution with a linear gradient of 0.3–0.6 M NaCl (HiTrap Q and AKTA purifier, GE healthcare). The purified tRNA[fMet] was charged with methionine by incubating with MetRS and ATP at 37°C for 30 min, and isolated with the anion exchange resin (Q-Sepharose HP, GE healthcare) at pH 4.7. Methionyl-tRNA[fMet] was labeled with Cy5-SE (GE health-care) on ice for 1 h in 40 mM phosphate buffer (pH 9.1), and recovered with the anion exchange resin (Q-Sepharose HP, GE health-care) at pH 4.7. Cy5-Met-tRNA[fMet] was precipitated with ethanol and dissolved in 20 mM potassium acetate. The concentration of Cy5-Met-tRNA[fMet] was determined from A_{260}. To label translation products, 6.6 x 10^{-4} A_{260} units Cy5-Met-tRNA[fMet] was added per μL of PUREfrex reaction mixture.

The S30 extract-based *in vitro* translation was performed using *E. coli* S30 Extract System for Linear Templates (Promega) accord-ing to the manufacturer's instructions in the presence of ^{35}S-methionine. Mutant ribosomes (ΔbL31) purified as described[61] were used where indicated. ArfA, ArfB, EF-G and its Δdomain IV mutant were purified as described.[31,62] DNA templates were prepared by PCR, as summarized in Table S4. The reaction mixture was treated with 1 μM of purified Pth for 10 min at 37°C, or 200 μg/mL of puromycin for 5 min at 37°C where indicated. The reaction was stopped by dilution into an excessive volume of 5% TCA. After standing on ice for at least 10 min, the samples were centrifuged for 3 min at 4°C, and the supernatant was discarded by aspiration. The precipitates were then vortexed with 0.9 mL of acetone, centrifuged again, and dissolved in SDS sample buffer (62.5 mM Tris-HCl, pH 6.8, 2% SDS, 10% glycerol, 50 mM DTT) that had been treated with RNAsecure (Ambion). Finally, the sample was divided into two portions, one of which was incubated with 50 μg/mL of RNase A (Promega) at 37°C for 30 min, and separated by a WIDE Range SDS-PAGE system (Nakalai Tesque).

β-galactosidase assay

E. coli cells harboring the *lacZ* reporter plasmid were grown overnight at 37°C in LB medium supplemented with 100 μg/mL ampicillin. On the next day, they were inoculated into fresh LB medium containing 2x 10^{-4}% arabinose and 100 μg/mL ampicillin. The cultures were allowed to grow at 37°C for approximately 2.5 h (A_{660} = ~0.2). Subsequently, the temperature was shifted to 42°C if indicated,

and growth continued until the A_{660} doubled. Afterward, 20 μL portions were subjected to a β-galactosidase assay as described.[21,22] Estimated miller units (*m.u.*) were subjected to the following formula to calculate the TC index (*in vivo*).

TC index (*in vivo*) = *m.u.*(DE/P⁺)/*m.u.*(no DEP)

TC indices were calculated from three independent biological replicates.

Sucrose density gradient ultracentrifugation of *in vitro* translation reaction mixture.

A PURE*frex* reaction mixture (25 μL at 37°C or 50 μL at 20°C) in the presence of Cy5-Met-tRNA^fMet was mixed with 100 μL of TNM buffer (25 mM Tris-HCl, pH 7.6, 100 mM NH₄Cl, 10 mM MgCl₂, 1 mM DTT), and centrifuged at 20,000 x g for 10 min at 4°C. The supernatant was recovered, layered on the top of a 10–30% sucrose gradient containing TNM buffer in Open Top Polyclear Centrifuge Tubes (14 × 89 mm, SETON) and centrifuged at 39,000 rpm for 3 h at 4°C (Beckman OptimaL-90K, SW41-Ti). Fractions were obtained (each fraction, ~350 μL) using a Gradient Station (BIOCOMP) equipped with a MICRO COLLECTOR AC-5700 (ATTO). The ribosome distribution was monitored by A_{254} measurements, using a BIO MINI UV MONITOR (AC-5200S, ATTO). Each fraction was mixed with an equal volume of 10% TCA and processed for 11% WIDE Range Gel SDS-PAGE, as described above. Fluorescent translation products were detected by an Amersham Typhoon scanner RGB system (GE Healthcare) using a 635 nm excitation laser and an LPR emission filter.

IRD reconstitution using the isolated 70S complex

A PURE*frex* reaction mixture (150 μL at 20°C for 1 h, performed with A19 ribosome) in the presence of Cy5-Met-tRNA^fMet was mixed with 150 μL of TNM buffer, and centrifuged at 20,000 x g for 10 min at 4°C. The supernatant was recovered and fractionated by sucrose gradient centrifugation, as described above. The fractions containing the 70S complex were withdrawn, frozen in liquid nitrogen, and stored as "isolated 70S" at −80°C.

The isolated 70S fraction was mixed with 12% PURE buffer (final 50 mM HEPES-KOH, pH 7.6, 100 mM K-Glu, 2 mM spermidine, and 1 mM DTT) and incubated on ice for at least 5 min. The final Mg^{2+} concentrations were 20 mM in Figure 5 and 10 mM in Figure 6. Purified translation factors included within PURE*frex* were added where indicated. GTP was supplemented with an equal concentration of MgCl₂ to counteract the Mg^{2+}-chelation, and mixed with the isolated 70S at a final 1 mM concentration. The purified Pth was added (final 1 μM) at the initiation of the incubation or after the incubation as indicated, and further incubated for 20 min at 4°C or 37°C. Purified IF3, EF-G and RRF, were mixed with the isolated 70S at 1 μM each.

For SDG fractionation of the isolated 70S after the incubation assay, 80 μL of the reaction sample was mixed with 120 μL of TNM buffer and analyzed as described above. When indicated, 10 μL of translation factors mix in PURE*frex* v1.0 system was added.

Ribo-seq analysis

Ribo-seq data in the presence or absence of RRF were downloaded from GSE151688.[34] Adaptor sequences were trimmed from raw reads with the use of cutadapt. Reads with low quality were discarded with the use of fastq_quality_trimmer and fastq_quality_filter of the FASTX-Toolkit. Ribosomal RNA reads were removed by alignment with rRNA sequences with the use of Bowtie version 2.2.5, and the remaining reads were aligned to the *E. coli* MG1655 genome with the use of Hisat2. Multiple mappings were allowed. Metagene analysis was performed with a custom Python script and with the use of Numpy (v1.17.3) and Pysam (v0.15.3).[63] For genes with each indicated sequence motif, normalized reads mapped around the motif were summed.

QUANTIFICATION AND STATISTICAL ANALYSIS

Statistical analyses

Statistical analyses were conducted by using the software R (https://www.r-project.org).

The average of three independent experiments (n = 3) with standard error (SE) value are shown. We did not use any methods to determine whether the data met the assumptions of the statistical approach.

Quantification of the signals from gel images
IRD frequency in vitro

The ratio of the translation-completed chain (full length: FL) against Pth-sensitive polypeptidyl-tRNAs (pep-tRNAs), which signifies the occurrence of IRD-induced abortion in the total *in vitro* translation products, was calculated as the translation continuation (TC) index. In detail, the radioactivity (^35S-methionine) or Cy5-fluorescence proportion of "FL" and "pep-tRNA" among the samples with neither Pth- nor RNase-treatment was quantified by the Multi Gauge software (Fujifilm), and the IRD frequency (in %) is obtained by the following formula.

IRD frequency (*in vitro*) = (pep-tRNA)/[(FL) + (pep-tRNA)]

In case of S30 extract-based experiments, IRD frequency is obtained by the following formula.

IRD frequency (S30) = (truncate)/[(FL) + (truncate)]

The average of three independent experiments is presented with standard error (SE) value.

Proportions of peptidyl-tRNAs that are sensitive to puromycin/Pth

First, the ratios of the peptidyl-tRNA in the samples were calculated with the following formula.

Pep-tRNA = (pep-tRNA)/[(FL) + (pep-tRNA)]

The peptidyl-tRNA that is sensitive to puromycin or Pth was then calculated with the following formula.

Pep-tRNA (Pm^S) = 100 – [pep-tRNA(Puromycin-treated)/pep-tRNA(control)] x100.

Pep-tRNA (Pth^S) = 100 – [pep-tRNA(Pth-treated)/pep-tRNA(control)] x 100.

Distribution of pep-tRNA in the SDG analysis

The distribution of peptidyl-tRNA in each fraction was normalized by the following formula.

Distribution of pep-tRNA (fraction X) = [pep-tRNA(fraction X)/pep-tRNA(sum of all fractions)] x 100.